Supporting Information Appendix

Ponti et al. 10.1073/pnas.1314437111

Fine scale ecological and economic assessment of climate change on olive in the Mediterranean Basin reveals winners and losers

Luigi Ponti[1,2,*], Andrew Paul Gutierrez[2,3], Paolo Michele Ruti[4], Alessandro Dell'Aquila[4]

[1]Laboratorio Gestione Sostenibile degli Agroecosistemi, Agenzia nazionale per le nuove tecnologie, l'energia e lo sviluppo economico sostenibile (ENEA), Centro Ricerche Casaccia, Via Anguillarese 301, 00123 Roma, Italy.
[2]Center for the Analysis of Sustainable Agricultural Systems (CASAS), Kensington, CA 94707, USA (Website: http://CASASGLOBAL.org); e-mail: casas.global@berkeley.edu (APG).
[3]College of Natural Resources, University of California, Berkeley, CA 94720, USA.
[4]Laboratorio Modellistica Climatica ed Impatti, ENEA Centro Ricerche Casaccia,Via Anguillarese 301, 00123 Roma, Italy; e-mails: paolo.ruti@enea.it (PMR); alessandro.dellaquila@enea.it (ADA).
*Corresponding author: Luigi Ponti, ENEA Centro Ricerche Casaccia, Edificio T13, Sacco Postale 101, Via Anguillarese 301, 00123 Roma, Italy; e-mail: luigi.ponti@enea.it; phone: +39 06-3048-6459; fax: +39 06-3048-6308.

SI Discussion

Approaches for Estimating the Impact of Weather and of Climate Change on the Distribution and Abundance of Species. The recent literature speaks clearly to the urgent need for approaches to estimate the geographic distribution and relative abundance of species that experience novel climates due to range expansion or as a consequence of climate change (see refs. 1, 2-9). Specifically, Section 4.3 ("Assumptions about future trends") by Working Group 2 in the fourth assessment report (AR4) of IPCC outlines the shortcomings of widely used standard methods based largely on the climate envelope approaches (i.e., ecological niche models, ENMs) used to assess the impact of climate change on ecosystems (10). Among the gaps identified in IPCC AR4 were the inability to account for species interactions, the lack of physiological mechanisms, and the inability to account for population processes (11). These shortcomings were evident in the earliest ENM applications on a geographic scale by APG (12). Including multitrophic interactions in assessments of climate effects on biological systems has been an ongoing major challenge (13-19). Species interactions constrain the geographic range of species even on an evolutionary time scale (20) and play a key role in host-parasite relationships in general (21). Recent advances have been based on species interaction indices (22) and species co-occurrence matrices (23, 24). All of these correlative ENMs make implicit ecological and mathematical assumptions that have no mechanistic basis for the biology, making the results and their transferability conjectural with the predictive power potentially lower than spatial interpolation (25).

Other approaches in the literature have attempted to integrate physiological mechanisms and population processes in climate impact assessments (26-31). These methods are substantially closer to the correlative end of the process-correlation model continuum (32) and are part of an ENM methodological base used in such analyses (9, 33, 34). Hybrid models superimpose population dynamics layers on correlative approaches with an associated substantial increase in model complexity and computational burden (35). Recent integration of mechanistic models with economic analysis have used stochastic population dynamics models lacking mechanistic underpinnings (36).

In contrast, the physiologically-based demographic system model (PBDM) used here explicitly captures the mechanistic weather-driven biology and dynamics of olive and olive fly. In general, PBDMs (see also ref. 37) predict the weather-driven phenology, dynamics and distribution of species across wide geographic areas on a daily basis – a time step rarely used in macroecological modeling (29). More generally, PBDMs can also include other interacting species in this (e.g., olive/olive scale and its parasitoids) and other food chains or webs (38). The model captures via sub-models the processes of resource acquisition and allocation (i.e., the metabolic pool model, see ref. 39), and the birth-death rates. PBDMs are sufficiently detailed to be realistic, and yet complexity is kept to a minimum by applying the same dynamics model and process sub models to all trophic levels (40, 41). The complexity enters the model at the conceptual level and running the model requires minimal computational capacity. These models have contributed to basic theory and helped solve many applied field problems because they bridge the gap between purely theoretical analytic models and overly complicated simulation models (42). PBDMs have been successfully applied across trophic levels and taxa in various ecosystems and geographic regions, and through time. The underlying conceptual model was the basis for developing novel economic theory (43). The biological processes governing the dynamics of olive and olive fly are modeled explicitly, and the model is used as the production function in the bioeconomic analysis to capture the effects of weather on the biological system (see 44). Physiological analogy across trophic levels (see also refs. 45, 46) is a powerful conceptual tool as used here, and is currently considered as a way to tackle the huge challenges facing global ecosystem modeling (47).

We note however that despite shortcomings, in many cases ENMs are the only available option for estimating the ecological niche (48) of invasive species, and may provide a useful approximation if the results are interpreted with due consideration of the limitations of the models (49).

The Mediterranean Basin and Climate Change. The Mediterranean Basin is a climate change hotspot of global relevance (50, 51). This consensus was reached using different climate models predicting climate change for the Mediterranean region (50, 52). However, relative to the rest of the globe, the uncertainty associated with the predictions of the different models implementing the A1B climate scenario is low (53). This means that climate change signals for the Mediterranean region are robust across forcing scenarios, future time periods, and a range of global and regional climate models, with the magnitude of the signal increasing with the intensity of forcing (54). Our implementation of the A1B scenario entails a 1.8°C average warming across the Basin in the period 2041-2050 using 1961-1970 as the reference period (55). This scenario is part of an innovative multi-model system developed within the European project CIRCE (Climate Change and Impact Research: the Mediterranean Environment) to produce high-resolution, realistic simulations of regional climate via an

improved representation of the Mediterranean Sea for use in impact assessments (53). For the first time, realistic net surface air-sea fluxes are available that are key to simulating regional climate and impacts in the Basin (56). CIRCE climate projections are overall consistent with the findings obtained in previous scenario simulations (e.g., PRUDENCE, ENSEMBLES and CMIP3), and this suggests that projections for the Mediterranean region are robust to substantial changes in the configuration of the climate models (53). The use of intermediate climate change as projected under A1B is a standard reference practice in IPCC AR4 and in the climate impacts literature. The A1B scenario is towards the middle of the IPCC range of GHG forcing scenarios, with A2 being close to the high end but showing small average difference from A1B (smaller than the standard deviation of mean warming in our A1B scenario, see ref. 55) for the Mediterranean Basin within the 2050 time horizon considered in our analysis (57).

Validation of the Olive/Olive Fly PBDMs. Models that lie at the opposite ends of the process-correlation continuum are tested in different ways (32) according to their intended purpose (58). Because correlative ENMs are based on species presence-absence records, their projections implicitly include an undefined number of biotic and abiotic factors that determine observed species distribution (59), and hence it is possible to test them against an additional set of species records and to quantify predictive performance. However, species records are both input and output of correlative ENMs and while this makes validation appear easier, this comes at the expense of accuracy. ENMs are essentially correlative devices with no knowledge of the mechanisms underlying the patterns they predict (60), and using an ensemble of ENMs may be the only option to reduce uncertainty (60, 61). At the opposite end of the process-correlation continuum are PBDMs that do not begin with the assumed native range of a species based on distribution records, but rather, model the biology (physiology) and population dynamics of the target species and other species in the same food chain or web (i.e., the system). This biology when driven by weather allows prediction of the phenology, dynamics and distribution of the interacting species using extant and climate change weather across wide geographic areas independent of distribution records (62, 63) with higher accuracy and at a finer scale than ENMs. PBDMs may be viewed as time-varying life-tables (*sensu* ref. 64) that include the important factors that determine observed species distribution (see also ref. 65) – factors that can be modeled in a mathematically explicit form based on laboratory and field data.

The goal of our analysis was not precise prediction of olive yield across the Mediterranean Basin as this is unrealistic due to the combined effects of factors such as a plethora of local varieties and agronomic practices (e.g., age structure, planting densities, nutrients and water). Furthermore, no suitable yield records are available for validation. Bloom date is the major factor determining season length and potential yield (66-69), and this was well captured by the model. For example, the model was tested against field data from a previous detailed study for the island of Sardinia (70) where it reliably predicted (e.g., through time) the bloom date of olive. The predictions were validated using a set of 94 Sardinian olive groves monitored by the local agricultural extension service ERSAT (Dr. Q.A. Cossu). A sub set of 21 paired weather station/olive grove were selected to allow a one-to-one comparison with no duplications, and to minimize the distance between the weather station and the olive grove. The analysis showed that at the scale of Sardinia, the important factors explaining most of the discrepancy between observed and simulated olive bloom dates

were: elevation differences between the olive grove and its paired weather station, and whether the station and the olive farm were on the same slope. All of these factors affect local microclimate. Detection of these differences was a clear indication of how sensitive and reliable the model is. Similarly, the model detected the production of olive in the microclimates along the northern Italian lakes and explained the distribution of olive fly in California and Arizona (71).

We side stepped the issue of yield prediction in this study by simulating the effects of climate on olive meta-physiology, and used a normalized measure to scale the observed yield at each grid point. The effects of the above factors and others on yield across the Basin are subsumed in the historical yield records obtained from a state of the art, widely used seven-year average dataset for the global geographic distribution of yields for 175 crops centered on the year 2000 (72). The relative physiological effects on changes in olive yield due to climate change were estimated using the weather-driven PBDMs that summarize the extensive data in the literature (71). The relative changes in olive yield (simulated physiological effect) predicted by the model using weather data from climate model scenarios between the two periods 1961-1970 and 2041-2050 were scaled to the overall range of yield change across all locations (Eq. 1 in the manuscript), and used to estimate the local changes in yield due to climate change. The use of relative yield change (simulated physiological effect) and multi-year average data (observed data) enabled a robust estimate of the relative magnitude and direction of yield change for olive under projected climate warming across the Basin. To estimate this in a tri-trophic context is considered the greatest single challenge for reliably assessing ecosystems under climate change (18). Hence, while data to ground truth the analysis is desirable, olive yield data were not available. This is a short coming that all modeling approaches face (see e.g., ref. 73).

In general, our PBDM for olive and olive fly is more heuristic than predictive, due to constraints of available data for testing the model, and for improving its biological detail. But this is also the case for ENMs (74-76) that ideally require meta-analysis of multiple models to derive reasonable projections under climate change (60). Despite this, PBDMs have proven sufficiently accurate to allow a wide range of successful applications in agroecosystem management (e.g., ref. 41). This is possible because PBDMs model the species' biology explicitly, and hence provide (at least qualitatively) accurate predictions of potential spatio-temporal patterns of say olive yields across large geographic areas (70, 71) without the transferability issues typical of ENMs (77, 78). The olive PBDM explicitly captures the growth and fruiting biology of olive included implicitly in regression models commonly used to forecast olive yields locally (79) based on records of flowering events and weather (80-87). This capacity increases confidence that our approach to scale observed yield using simulated net yield change is at least qualitatively accurate across the Basin. Yield forecast models are based on pre-peak airborne pollen concentration that functions as a synthetic index describing weather patterns prior to flowering (88, 89), as pollen emission records include information about the relationships between fertilization and successive fruit setting (84, 85, 90, 91). However, the causal relationships are not included in yield forecast models, and hence yield prediction models have only local validity (79). In contrast, the olive PBDM includes these causal relationships explicitly, and is able to account for post-flowering factors that influence fruit growth not included in most yield forecast models (81). For this reason, PBDMs give regionally accurate projections of the favorability for relative olive growth and yield across the Basin.

Olive is the basis of the Mediterranean rain-fed agroforestry system (92), one the oldest (93-96), most ecologically-sustainable rain-fed agroecosystems worldwide (97), and as such provides a model to design sustainable rain-fed systems for the semiarid Africa (92), including regions such as the Sahel (98). Olive is a well-documented cosmopolitan (agro) ecosystem, and its economic viability and persistence have important implications for preventing and ameliorating desertification that is a major environmental threat to the whole Mediterranean region (99-103). Its economic and social viability and its persistence are important for preventing soil loss, especially on sloping land (104-107), combating desertification (92, 97), reducing fire risk (106, 108, 109), and conserving biodiversity (106, 107, 110, 111) under global climate change. The olive/olive fly system is also a suitable case study exemplifying the importance of including trophic interactions when assessing biological and economic impacts of climate change over large geographic areas such as the Mediterranean Basin, and it could be a template for formulating models for assessing extant and climate change impact in other agroecosystems (e.g., grape, citrus, etc.) and their extant pests and potential invasive species (112, 113). Furthermore, the focus on regional impacts and the socio-economic dimensions of climate change is central to the forthcoming IPCC fifth assessment report (see http://www.ipcc.ch/report/ar5/).

Overview on Agricultural Policy Relevant to Olive Production. This section provides an overview on the regulatory, support and subsidy framework for olive oil in the European Union (EU) that puts the results of our study in a wider policy context. It is important to note that agricultural policy is negotiated among and common to all EU member countries (the Common Agricultural Policy, CAP). Olive oil production is highly regulated by CAP (114), and this impacts olive production substantially as most of the crop is used to produce olive oil in Europe (International Olive Council, http://www. internationaloliveoil.org/) where about 80% of olive oil is produced, and where roughly one third of farmers grow olive (115). Since the 1960s, the main CAP tool to support olive farmers has been via subsidy directly linked to olive oil production; policy that favors intensive, less ecologically-sustainable olive production systems (103, 116). Intensification mostly occurs on large farms that can more easily afford the new investments in technology (e.g., irrigation), whereas small growers in marginal areas with old, less productive trees and no access to irrigation are penalized and many abandon these traditional olive systems (116-119). A change in policy support is needed that would favor extensive, traditional systems mostly associated with cultural landscapes of high biodiversity (120). The 2003 CAP reform started decoupling the link between the amount of olive oil produced and the size of subsidy received by farmers (109), and beginning in 2005 increasing emphasis has been given to environmental compliance as olive growers will only be entitled to subsidies if they comply (i.e., the so-called cross-compliance, see ref. 102) with a set of sustainable agricultural practices defined by each EU country (e.g., cover crops to control soil erosion, see ref. 121). However, many existing intensive olive plantations maintain high-input farming practices likely due to path dependency that results from structural changes (e.g., high planting density) induced during the past decades by a massive increase in EU subsidies peaking to about 1.3 Euros per liter of oil in 2003 (115). By contrast, small olive farmers with the greatest environmental stewardship potential, are also those most likely to abandon their groves under the current subsidy regime that fully decouples subsidy and production with mandatory implementation of environmental cross-compliance (103). Ongoing CAP reform for the period 2014-2020 is considering a specific support scheme for

small farmers aimed to address prior distortion (122). Finally we note that country-specific agricultural policies supportive of olive farming have also been in place in North Africa and the Middle East but never in the form of direct subsidies to olive oil production as occurred in the EU (123).

In the span of two decades, olive oil turned from a niche product into an important component in the diets of developed countries (123), and yet the rapid industrialization of olive production with the associated conversion of vast Mediterranean landscapes to olive monocultures (124, 125) resulted in a range of environmental pressures (126) mostly driven by high CAP subsidies with the feedback loops within production and consumption systems playing a minor role (115). However, aggregate supply effects with subsequent market changes may occur in the future as a result of spatial and temporal shifts in olive production as driven by climate change. Different countries may accrue typical supply/demand ratios that influence olive oil prices, with the quality of oil currently being particularly important in determining price across countries (127). Market-induced price changes were not included in our analysis.

SI Materials and Methods

Geographic Distribution of Olive. Despite olive's prime importance in the Basin (107), published GIS maps of its distribution were unavailable. Hence to produce a nearly continuous map of the *potential* olive growing area at the Mediterranean scale, data and maps from various sources were smoothed using the v.kernel module of GRASS (128). The resultant map amalgamates data from the following sources: Corine satellite-derived land cover database (http://www.eea.europa.eu/data-and-maps/data/corine-land-cover-2000-clc2000-seamless-vector-database); M3-Crops Data for olive (http://www.sage.wisc.edu/) (72); FAO (Food and Agriculture Organization of the United Nations) Agro-MAPS (http://kids.fao.org/agromaps/) and GAEZ data (Global Agro-Ecological Zones; see http://gaez.fao.org/); published data and printed maps of olive distribution (e.g., 95, 96, 129). The M3-Crops data for yield are representative of the year 2000, and proved crucial for estimating the distribution in the southern Mediterranean Basin where Corine data for olive were not available. The M3-Crops Data refer to political units at variable levels of detail: county (e.g., Tunisia and Egypt), state (Algeria, Jordan, and Lebanon), or whole country (Morocco, Libya, Israel, Palestine, and Syria). The general approach to reconciling discrepancies between the data sets was to first use the satellite-derived land cover class for olive groves (Corine) where available, and then resort to datasets that derive olive distribution indirectly from agricultural statistics and the global satellite-derived distribution of cultivated land (M3-Crops). Published reports, maps and other available records were used as checks on the accuracy of our map. The percentage distribution of olive in the various FAO ecological zones of the Basin (130) was estimated using the GRASS/R interface module spgrass6 (131).

The System Model. Conceptually, our mechanistic weather-driven physiologically-based demographic models (PBDMs) build on the idea that all organisms are consumers and all have similar resource acquisition functions and allocation priorities; a notion that allows use of the same resource acquisition model and birth-death dynamics models to describe explicitly the biology of heterotherm species across trophic levels (42, 132, 133), including the economic one (43) (see Fig. S2). The inflow and outflow processes are analogous across species and have similar shapes described by the same functions. Resource acquisition (i.e.

the supply, *S*) is a search process driven by organism demand (*D*), with allocation occurring in priority order to egestion, conversion costs, respiration, and reproduction, growth, and reserves (40, 132, 134).

The development of PBDMs for plants is well established in the literature (135) with an excellent detailed example for coffee reported by Rodríguez *et al*. (136). These plant model provide a realistic base for linkages to herbivore and higher trophic levels (e.g., ref. 134). This is the structure used to model olive and olive fly dynamics (for details, see ref. 70 and SI Mathematical structure of the olive/olive fly model). The olive PBDM is a plant canopy model with subunit populations of leaves, stem, root and healthy and attacked fruit that allow capture of the bottom-up plant effects on olive fly dynamics (Fig. 1). The model simulates the age-mass structured population dynamics of nine functional populations (n = 1…9): olive leaf mass and numbers {sub models n=1, 2}, stem plus shoots {n=3}, root {4} and fruit mass and number {5, 6} that are linked via photosynthate supply and demand consideration, The models for immature olive fly in fruit {7}, and reproductive and dormant fly adults {8, 9} are similar, except that for convenience we follow only the number dynamics.

The developmental rates of olive and the fly depend on temperature and are captured by the non-linear model proposed by Briére *et al.* (137). The time step in the model is a day of variable length in physiological time units. Temperature influences nearly all aspects of olive's growth and the effects are captured by a function of temperature that is the normalized net of the photosynthetic and respiration rates. This function also defines the optimum temperature, and the upper and lower thermal thresholds for development. While the model predicts the growth and yield responses of olive to weather in substantial detail, local varieties, plant age structure, and agronomic practices across the Basin affect yield. The olive model predicts flowering phenology that is controlled by vernalization, age-structured mass growth and yield, and fruit mortality due to temperature, photosynthate shortfalls and the timing and rate of fly attack.

The biology of olive fly is closely linked to olive fruit age and availability. And though the fly lacks an obligate diapause, adult females may enter reproductive quiescence when host fruit are low and/or temperatures are high (see ref. 71). The model predicts the daily age structured dynamics of all life stages including the pattern of reproductive quiescence. As in olive, the effects of temperature on olive fly vital rates are captured by analogous functions for development, reproduction and mortality.

Critical to interpreting the results is that olive has wider thermal limits than olive fly, and this biology has pronounced effects on the crop-pest dynamics, and the economics of olive culture across the region.

Weather and Weather Scenarios. The olive/fly system dynamics are driven by daily weather [i.e., max-min temperature and solar radiation (W m^{-2} d^{-1})], and two weather scenarios are used: daily weather for the base period 1961-1970 (weather vector $\vec{w}_0$) and an A1B scenario with +1.8°C ± 0.3°C average warming for the period 2041-2050 (weather vector $\vec{w}_{+1.8}$) (see ref. 55). A weak negative trend is predicted for precipitation (55), and because olive is drought tolerant (66, 138), soil moisture is assumed non-limiting for olive culture in the current region of cultivation (see also refs. 139, 140). We note that irrigation is used in some areas of low rainfall (e.g., areas of Egypt and the province of Andalucía, Spain).

The weather data used in the study were estimated via regional downscaling of a global climate simulation (ECHAM5/MPI-OM) for the period 1951-2050 (55). The global weather

simulation was run at ~200 km grid resolution using observed [GHG] for years 1951-2000 and the IPCC A1B GHG emissions scenario for 2001-2050. Using this coarser global simulation as the boundary condition, a regional climate model (PROTHEUS) was used to refine and rescale the weather data to a 30 km grid resolution. PROTHEUS is a coupled atmosphere-ocean regional model that allows simulation of local extremes of weather via the inclusion of a fine scale representation of topography and the influence of the Mediterranean Sea (141). A subset of the PROTHEUS data for the periods 1961-1970 and 2041-2050 were used in our study performed on a 30 km grid.

Simulation and GIS Analysis. The same initial conditions were used for all 995 grid points in the analysis, but grid-point specific weather data were used to drive the model. For convenience, we ignore grid point coordinate in the equations. The model was run continuously across all locations for the periods 1 January 1960 to 31 December 1970 (weather data $\vec{w}_0$) and 1 January 2040 to 31 December 2050 ($\vec{w}_{+1.8}$). The model was assumed equilibrating to local weather during the first year at each grid point simulation, and hence the data for this year were not used to compute the summary means, standard deviations and coefficients of variations across years for each output variable. Welch's two-sample t-test (statistical software R, http://www.r-project.org/) was used to compare the simulation data for scenarios in five sub-regions of the Mediterranean Basin (see also Fig. S9). Changes in the variability of olive yield, fruit infestation by olive fly, and profit between scenarios $\vec{w}_0$ and $\vec{w}_{+1.8}$ were computed for yield as the difference in the coefficient of variation ($\Delta CV = CV_{+1.8} - CV_0$), and for olive fly infestation and profit as the difference in the interquartile range ($\Delta IQR = IQR_{+1.8} - IQR_0$). Yield and profit variability was computed using normalized simulated yields (Y_0 and $Y_{+1.8}$) to scale observed yields (Y_{obs}) so as to generate two sets of yearly values for the $\vec{w}_0$ and $\vec{w}_{+1.8}$ scenarios. Values used to compute CV are assumed to be always positive or null as is the case for yield (142), whereas CV has limitations when there are negative values and for proportions (143, 144), and hence we used IQR (i.e., the range for the middle 50% of the data) as an alternative measure of variability for fruit infestation and profit.

GRASS GIS (http://grass.osgeo.org/) was used to map the model output at all locations below 900m (145) using inverse distance weighting interpolation at 3-km resolution based on an Albers Equal Area conic projection. Base GIS layers used in the analysis are in the public domain: a digital elevation model from NOAA Global Land One-km Base Elevation (http://www.ngdc.noaa.gov/mgg/topo/globe.html); state boundaries and land cover coloring from Natural Earth (http://www.naturalearthdata.com/); Global Ecological Zones (130) from the GeoNetwork server (http://www.fao.org/geonetwork/). Histograms of the frequency distribution of output data for the different sub-regions of the Basin were produced using the R package ggplot2 (http://ggplot2.org/) (146). Statistical outliers were were identified using the R boxplot function (147, 148) and mapped as such to improve the visual presentation of data (149).

SI Mathematical Structure of the Olive/Olive Fly Model

The PBDM approach can model the individual or the average population. A canopy average plant model for olive (150) and a per capita model for olive fly (42, 132, 133, 151-154) were developed and used in our study.

To analyze the effects of weather on olive and olive fly, the per capita age-structured dynamics of growth, development, reproduction, and behavior as driven by weather and their interactions were modeled incorporating the underpinning biology and dynamics (see ref. 71). Common processes across trophic levels allow the same population dynamics and functional response models to be used to model the number and mass dynamics and interactions of olive and olive fly (155, see ref. 156, pp. 523-524). All biological processes are driven by weather making the model independent of time and place (157) cast in a demographic form (cf. refs. 42, 132). The details of our physiologically-based demographic model are outlined in this SI text and in greater detail in Gutierrez (42).

Population Dynamics. Our model simulates the age-mass structured population dynamics of nine functional populations (n = 1…9): the dynamics of olive leaf mass and numbers {models n=1, 2}, stem plus shoots {n=3}, root {4} and fruit mass and number {5, 6}, olive fly in fruit {7}, and reproductive and dormant adults {8, 9}.

The biology of resource acquisition and allocation is embedded in a distributed maturation time demographic model used to simulate the dynamics of age-mass structured populations (158) where time (t) and age (a) in the model are in physiological time units (see refs. 42, 71 for model values).

The general model for the ith age class of a population (e.g., for populations {1-6} and {8-9}) is

$$\frac{dN_i}{dt} = \frac{k\,\Delta a}{del}[N_{i-1}(t) - N_i(t)] - \mu_i(t)N_i(t). \qquad [S1]$$

N_i is the density of the ith cohort of consumer, k is the number of different age cohorts (stages), del is the expected mean developmental time, Δa is an increment in age physiological age, and $-\infty < \mu_i(t) < \infty$ is the proportional net loss rate that includes all age-species specific growth, birth, death and net immigration. The flow across all k age classes is depicted in Fig. S11A, and the pattern of emergence times for different values of Erlang parameter k are depicted in Fig. S11C. The parameter k in our model was assumed 40. Understanding [S1] and the role $\mu_i(t)$ plays is critical to comprehending the model's construction and functioning. Computing birth and growth rates requires the use of a functional response model.

A two dimensional distributed delay model is used for olive fly larvae because the eggs are deposited in fruit of different ages that continue to develop on the plant time scale (i), while the egg-larval stage continue to develop on the fly's time scale (j) (Fig. S11B). Note that net mortality of the ij^{th} age class ($-\infty < \mu_{i,j}(t) < \infty$) is also a component of this model but is not illustrated in Fig. S11B. Note that a cohort of eggs deposited on ith age fruit travels in the two dimensions.

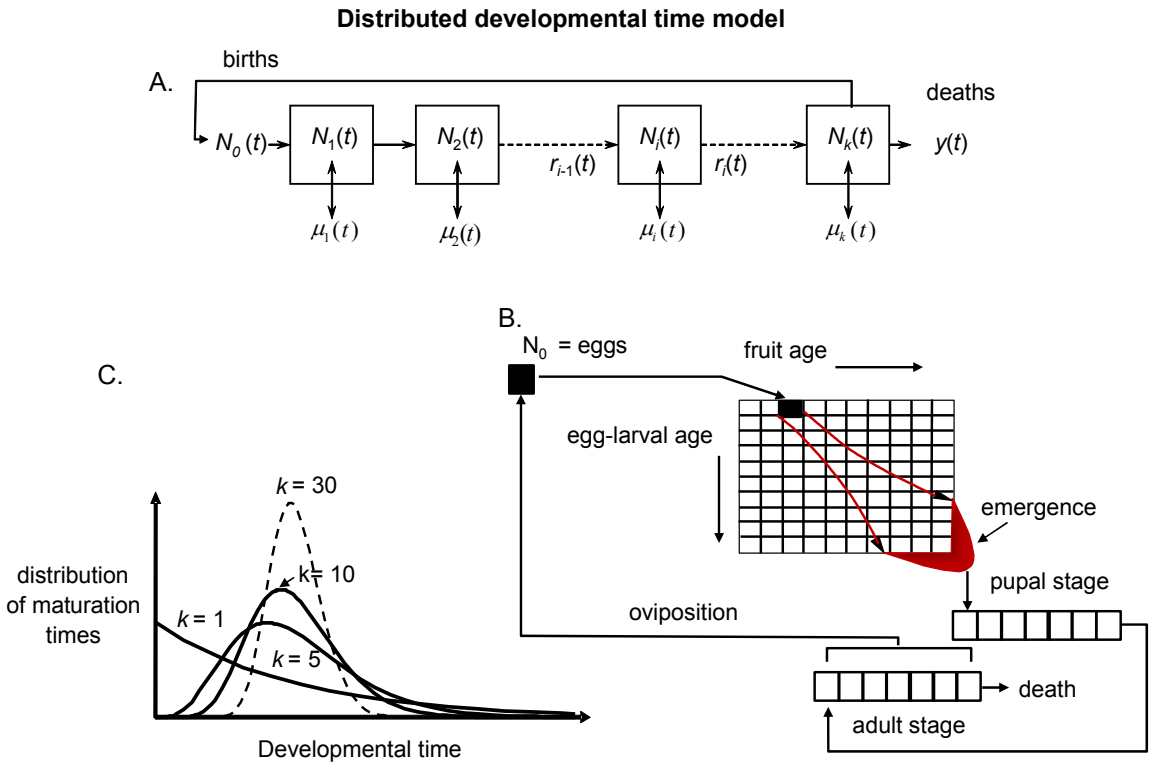

Fig. S11. (See text and ref. 71).

The Functional Response Model. A basic assumption of PBDMs is that all organisms (and sub-stages) are consumers (i.e., predators in a general sense, *N*), and all search (α) for resources (*X*). The same functional response model (Eq. S2) may be used to estimate search success for all consumers for multiple resources they may seek. For example, olive leaves search for light and the roots search the soil for water and nutrients, and adult olive flies seek olive fruit to deposit their eggs.

The per capita concave functional response model used for olive (Eq. S2) is similar to Watt's model (see ref. 42, p. 81). For olive fly we use the parasitoid form that allows multiple oviposition in the same fruit (i.e., the metabolic pool model; see refs. 39, 157).

$$S(u) = Dh(u) = D\left[1 - \exp\left(\frac{-\alpha X}{DN}\right)\right] \qquad [S2]$$

S(u) is the per capita resource acquired by consumers of population *N* in the face of intra-specific competition (i.e., the exponent) from resource *R*, *D* is the per capita demand rate, and α is the search rate. In olive, $\alpha(N) = 1 - \exp(-sN)$ is Beer's Law of plant physiology, *N* is the density of leaf area (or roots) each with per capita (unit) search rate *s*. This makes Eq. S2 a type III functional response. For olive fly, α was assumed constant because the aggregate search behavior is not known. However, to examine discrepancies at low densities of fruit (*O*), $\alpha(O) = 1 - exp(-sO)$ was used for α (see ref. 71).

In olive, with a known set of biological state variables (mass and age structure of plant subunits) and known temperature, light, water and nutrients, the quantity of photosynthate produced *S=S(u)* can be predicted using Eq. S2. This production is allocated first to egestion

(1−β), then respiration (i.e., Q_{10}), and after correction for conversion efficiency (λ) to reproduction and/or growth plus reserves (*GR*) (132).

$$GR = (S\beta - Q_{10})\lambda \qquad [S3]$$

We note that *S* depends on *D* in Eq. S2 that can be estimated under conditions of non-limiting resource by solving Eq. S3 and assuming $D \approx S_{max}$.

$$D \approx S_{\max} = \frac{\frac{GR_{\max(t)}}{\lambda} + Q_{10}}{\beta} \qquad [S4]$$

D is the sum of all plant subunit demands that may vary with age, stage, sex, size, temperature and other factors, and these and consumer preferences may be included in Eq. S2. Dividing both sides of Eq. S2 by *D* yields the consumers supply-demand ratio

$$0 \le \phi_{S/D} = S/D = h(u) < 1. \qquad [S5]$$

$\phi_{S/D}$ is used to scale per capita growth and fecundity from the maximum rate under optimal conditions (e.g., $GR = \phi^* GR_{\max}$). The allocation is made to the subunits as the fraction they contribute to the total demand (see ref. 42). In addition, if O(*t*) is the number of fruit susceptible to shedding, then at any time *t,* the number surviving fruit equals $O(t+1) = O(t)\phi_{S/D}(1-\mu_O(T))$.

We can model reproduction in olive fly in a similar manner. Observed per capita reproduction at optimal temperature *T** and age *x* may be modeled using an appropriate function ($F^*(x,T^*) = ax/b^x$) where *a* and *b* are fitted constants and $0 \le \phi_{OF}(T) \le 1$ corrects for the effects of observed temperature ($F(x,T) = F^*(x,T^*)\phi_{OF}(T)$; see Fig. S12A; cf. ref. 154, see also ref. 159).

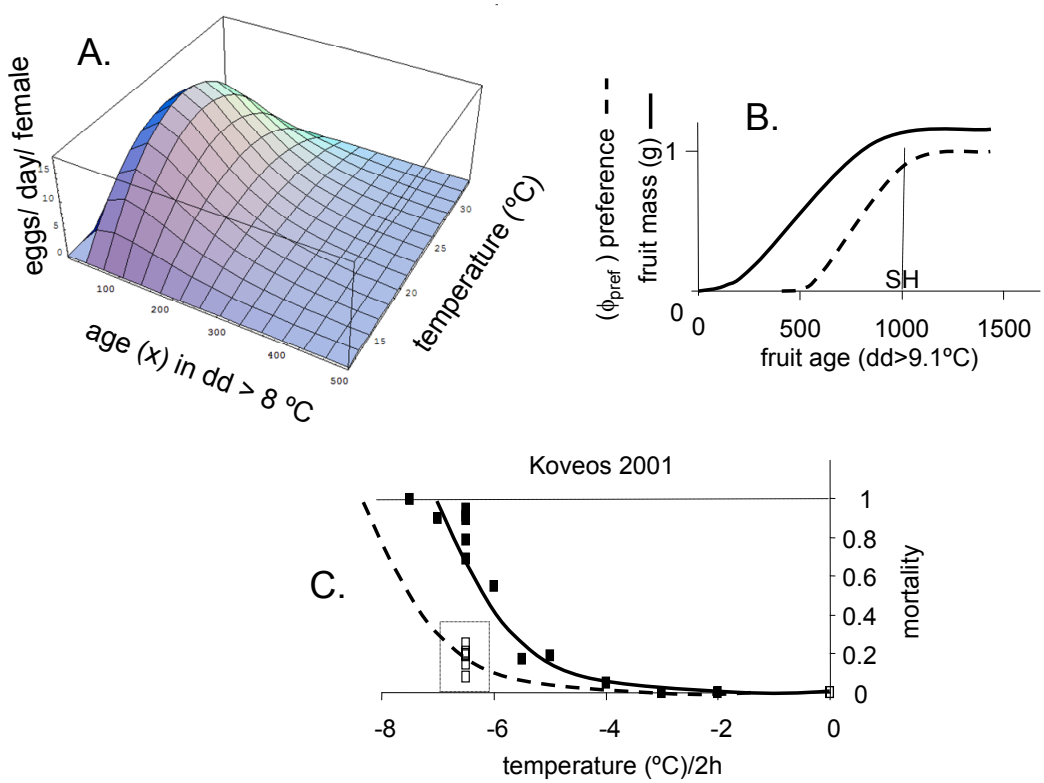

Fig. S12. (See text ref. 71).

The total population demand for oviposition sites by all adults $N_{OF}(T)$ is

$$D_{OF}(T) = \sum_{x=0}^{x_{max}} F(x,T) N_{OF}(x,T) .$$

The number of eggs (S) deposited in infested (O_I) and healthy fruit (O_H) not only depends on demand but also needs to be corrected for adult oviposition preference ($\phi_{pref}(x_{fruit})$, Fig. S12B) and search success. Substituting $D_{OF}(T)$ and $O = \phi_{pref(I)} O_I + \phi_{pref(H)} O_H$ in Eq. S2 yields total oviposition success $S(u,T) = \phi_{OF}(T) D_{OF} h(u,T)$ where α is the search rate. The relationship between olive fly oviposition preference and fruit growth and age are depicted in Fig. S12B where SH is the beginning of seed hardening.

The data on cold weather effects on olive fly mortality is scant, but the studies by Koveos (160) showed that some cold hardening occurs by exposure of adult flies to cool non lethal temperature for two hours and non exposure followed by exposure to various temperatures below zero. Fig. S12C summarizes Koveos's data with conditioning values indicated by the symbol (□) and non conditioning indicated by (■).

1. Roubicek AJ, et al. (2010) Does the choice of climate baseline matter in ecological niche modelling? *Ecol. Model.* 221(19), 2280-2286.
2. Barve N, et al. (2011) The crucial role of the accessible area in ecological niche modeling and species distribution modeling. *Ecol. Model.* 222, 1810-1819.
3. Veloz SD, et al. (2012) No-analog climates and shifting realized niches during the late quaternary: implications for 21st-century predictions by species distribution models. *Global Change Biol.* 18(5), 1698-1713.

4. Wiens JA, Stralberg, D, Jongsomjit, D, Howell, CA, & Snyder, MA (2009) Niches, models, and climate change: assessing the assumptions and uncertainties. *Proc. Natl. Acad. Sci. USA* 106(Supplement 2), 19729-19736.
5. Sinclair SJ, White, MD, & Newell, GR (2010) How useful are species distribution models for managing biodiversity under future climates? *Ecology and Society* 15, 8. http://www.ecologyandsociety.org/vol15/iss11/art18/.
6. Webber BL, Le Maitre, DC, & Kriticos, DJ (2012) Comment on "Climatic niche shifts are rare among terrestrial plant invaders". *Science* 338(6104), 193.
7. Guisan A, et al. (2012) Response to comment on "Climatic niche shifts are rare among terrestrial plant invaders". *Science* 338(6104), 193.
8. Petitpierre B, et al. (2012) Climatic niche shifts are rare among terrestrial plant invaders. *Science* 335(6074), 1344-1348.
9. Dawson TP, Jackson, ST, House, JI, Prentice, IC, & Mace, GM (2011) Beyond predictions: biodiversity conservation in a changing climate. *Science* 332(6025), 53-58.
10. Fischlin A, et al. (2007) in *Climate Change 2007: Impacts, Adaptation and Vulnerability. Contribution of Working Group II to the Fourth Assessment Report of the Intergovernmental Panel on Climate Change*, eds Parry, M. L., O.F. Canziani, Palutikof, J. P., van der Linden, P. J., & Hanson, C. E. (Cambridge University Press, Cambridge, UK), pp 211-272.
11. Elith J & Leathwick, JR (2009) Species distribution models: ecological explanation and prediction across space and time. *Annu. Rev. Ecol. Evol. Syst.* 40, 677-697.
12. Gutierrez AP, Nix, HA, Havenstein, DE, & Moore, PA (1974) The ecology of *Aphis craccivora* Koch and subterranean clover stunt virus in south-east Australia. III. A regional perspective of the phenology and migration of the cowpea aphid. *J. Appl. Ecol.* 11(1), 21-35.
13. Araujo MB & Luoto, M (2007) The importance of biotic interactions for modelling species distributions under climate change. *Global Ecol. Biogeogr.* 16(6), 743-753.
14. Davis AJ, Jenkinson, LS, Lawton, JH, Shorrocks, B, & Wood, S (1998) Making mistakes when predicting shifts in species range in response to global warming. *Nature* 391, 783-786.
15. Zarnetske PL, Skelly, DK, & Urban, MC (2012) Biotic multipliers of climate change. *Science* 336(6088), 1516-1518.
16. van der Putten WH, Macel, M, & Visser, ME (2010) Predicting species distribution and abundance responses to climate change: why it is essential to include biotic interactions across trophic levels. *Philosophical Transactions of the Royal Society B: Biological Sciences* 365(1549), 2025-2034.
17. Wardle DA, Bardgett, RD, Callaway, RM, & Van der Putten, WH (2011) Terrestrial ecosystem responses to species gains and losses. *Science* 332(6035), 1273-1277.
18. Tylianakis JM, Didham, RK, Bascompte, J, & Wardle, DA (2008) Global change and species interactions in terrestrial ecosystems. *Ecol. Lett.* 11(12), 1351-1363.
19. Guisan A & Thuiller, W (2005) Predicting species distribution: offering more than simple habitat models. *Ecol. Lett.* 8(9), 993-1009.
20. Pigot AL & Tobias, JA (2013) Species interactions constrain geographic range expansion over evolutionary time. *Ecol. Lett.* 16(3), 330-338.
21. Molnár PK, Kutz, SJ, Hoar, BM, & Dobson, AP (2013) Metabolic approaches to understanding climate change impacts on seasonal host-macroparasite dynamics. *Ecol. Lett.* 16(1), 9-21.
22. Sutherst RW, Maywald, GF, & Bourne, AS (2007) Including species interactions in risk assessments for global change. *Global Change Biol.* 13(9), 1843-1859.
23. Araújo MB, Rozenfeld, A, Rahbek, C, & Marquet, PA (2011) Using species co-occurrence networks to assess the impacts of climate change. *Ecography* 34(6), 897-908.
24. Wisz MS, et al. (2012) The role of biotic interactions in shaping distributions and realised assemblages of species: implications for species distribution modelling. *Biol. Rev.*, DOI 10.1111/j.1469-1185X.2012.00235.x.
25. Bahn V & McGill, BJ (2007) Can niche-based distribution models outperform spatial interpolation? *Global Ecol. Biogeogr.* 16(6), 733-742.
26. Morin X & Thuiller, W (2009) Comparing niche-and process-based models to reduce prediction uncertainty in species range shifts under climate change. *Ecology* 90(5), 1301-1313.
27. Kearney MR, Wintle, BA, & Porter, WP (2010) Correlative and mechanistic models of species distribution provide congruent forecasts under climate change. *Conservation Letters* 3(3), 203-213.
28. Keith DA, et al. (2008) Predicting extinction risks under climate change: coupling stochastic population models with dynamic bioclimatic habitat models. *Biol. Lett.* 4(5), 560-563.

29. Morin X & Chuine, I (2005) Sensitivity analysis of the tree distribution model PHENOFIT to climatic input characteristics: implications for climate impact assessment. *Global Change Biol.* 11(9)**,** 1493-1503.
30. Diamond SE, et al. (2012) A physiological trait-based approach to predicting the responses of species to experimental climate warming. *Ecology* 93(11)**,** 2305-2312.
31. Hulme PE & Barrett, SCH (2013) Integrating trait- and niche-based approaches to assess contemporary evolution in alien plant species. *J. Ecol.* 101(1)**,** 68-77.
32. Dormann CF, et al. (2012) Correlation and process in species distribution models: bridging a dichotomy. *J. Biogeogr.* 39**,** 2119-2131.
33. Higgins SI, O'Hara, RB, & Römermann, C (2012) A niche for biology in species distribution models. *J. Biogeogr.* 39(12)**,** 2091-2095.
34. Marion G, et al. (2012) Parameter and uncertainty estimation for process-oriented population and distribution models: data, statistics and the niche. *J. Biogeogr.* 39(12)**,** 2225-2239.
35. Dullinger S, et al. (2012) Extinction debt of high-mountain plants under twenty-first-century climate change. *Nature Clim. Change* 2(8)**,** 619-622.
36. Wintle BA, et al. (2011) Ecological-economic optimization of biodiversity conservation under climate change. *Nature Clim. Change*.
37. Holst N & Ruggle, P (1997) A physiologically based model of pest-natural enemy interactions. *Exp. Appl. Acarol.* 21(6/7)**,** 325-341.
38. Gutierrez AP, Ponti, L, & Gilioli, G (2010) in *Handbook of climate change and agroecosystems: impacts, adaptation, and mitigation*, eds Hillel, D. & Rosenzweig, C. (Imperial College Press, London, UK), pp 209-237.
39. Petrusewicz K & MacFayden, A (1970) *Productivity of terresrtial animals: principles and methods* (Blackwell, Oxford, UK).
40. Gutierrez AP, Mills, NJ, Schreiber, SJ, & Ellis, CK (1994) A physiologically based tritrophic perspective on bottom-up-top-down regulation of populations. *Ecology* 75(8)**,** 2227-2242.
41. Gutierrez AP & Ponti, L (in press) Eradication of invasive species: why the biology matters. *Environ. Entomol.*
42. Gutierrez AP (1996) *Applied population ecology: a supply-demand approach* (John Wiley and Sons, New York, USA).
43. Regev U, Gutierrez, AP, Schreiber, SJ, & Zilberman, D (1998) Biological and economic foundations of renewable resource exploitation. *Ecol. Econ.* 26(3)**,** 227-242.
44. Pemsl DE, Gutierrez, AP, & Waibel, H (2008) The economics of biotechnology under ecosystem disruption. *Ecol. Econ.* 66(1)**,** 177-183.
45. Gillooly JF, Brown, JH, West, GB, Savage, VM, & Charnov, EL (2001) Effects of size and temperature on metabolic rate. *Science* 293(2248-2251).
46. Gillooly JF, Charnov, EL, West, GB, Savage, VM, & Brown, JH (2002) Effects of size and temperature on developmental time. *Nature* 417(6884)**,** 70-73.
47. Purves D, et al. (2013) Ecosystems: Time to model all life on Earth. *Nature* 493(7432)**,** 295-297.
48. Warren DL (2012) In defense of 'niche modeling'. *Trends Ecol. Evol.* 27(9)**,** 497-500.
49. Pearson RG & Dawson, TP (2003) Predicting the impacts of climate change on the distribution of species: are bioclimate envelope models useful? *Global Ecol. Biogeogr.* 12(5)**,** 361-371.
50. Giorgi F (2006) Climate change hot-spots. *Geophys. Res. Lett.* 33**,** L08707.
51. Diffenbaugh NS, Pal, JS, Giorgi, F, & Gao, X (2007) Heat stress intensification in the Mediterranean climate change hotspot. *Geophys. Res. Lett.* 34**,** L11706.
52. Diffenbaugh N & Giorgi, F (2012) Climate change hotspots in the CMIP5 global climate model ensemble. *Climatic Change* 114(3)**,** 813-822.
53. Gualdi S, et al. (2012) The CIRCE simulations: a new set of regional climate change projections performed with a realistic representation of the Mediterranean Sea. *B. Am. Meteorol. Soc.***,** DOI 10.1175/BAMS-D-1111-00136.
54. Giorgi F & Lionello, P (2008) Climate change projections for the Mediterranean region. *Global Planet. Change* 63(2-3)**,** 90-104.
55. Dell'Aquila A, et al. (2012) Effects of seasonal cycle fluctuations in an A1B scenario over the Euro-Mediterranean region. *Climate Res.* 52**,** 135-157.
56. Dubois C, et al. (2011) Future projections of the surface heat and water budgets of the Mediterranean Sea in an ensemble of coupled atmosphere–ocean regional climate models. *Clim. Dynam.***,** DOI 10.1007/s00382-00011-01261-00384.

57. Giorgi F & Bi, X (2005) Updated regional precipitation and temperature changes for the 21st century from ensembles of recent AOGCM simulations. *Geophys. Res. Lett.* 32(21)**,** L21715.
58. Oreskes N, Shrader-Frechette, K, & Belitz, K (1994) Verification, validation, and confirmation of numerical models in the earth sciences. *Science* 263(5147)**,** 641-646.
59. Soberón J & Nakamura, M (2009) Niches and distributional areas: Concepts, methods, and assumptions. *Proc. Natl. Acad. Sci. USA* 106(Supplement 2)**,** 19644-19650.
60. Araújo MB, Whittaker, RJ, Ladle, RJ, & Erhard, M (2005) Reducing uncertainty in projections of extinction risk from climate change. *Global Ecol. Biogeogr.* 14(6)**,** 529-538.
61. Thuiller W (2007) Climate change and the ecologist. *Nature* 448(2)**,** 550–552.
62. Gutierrez AP, Ponti, L, d'Oultremont, T, & Ellis, CK (2008) Climate change effects on poikilotherm tritrophic interactions. *Climatic Change* 87**,** S167-S192.
63. Gutierrez AP & Ponti, L (in press) in *Invasive Species and Global Climate Change*, eds Ziska, L. H. & Dukes, J. S. (CABI Publishing, Wallingford, UK).
64. Gilbert N, Gutierrez, AP, Frazer, BD, & Jones, RE (1976) *Ecological relationships* (W.H. Freeman and Co., San Francisco, USA).
65. Radchuk V, Turlure, C, & Schtickzelle, N (2013) Each life stage matters: the importance of assessing the response to climate change over the complete life cycle in butterflies. *J. Anim. Ecol.* 82(1)**,** 275-285.
66. Connor DJ & Fereres, E (2005) The physiology of adaptation and yield expression in olive. *Hortic. Rev.* 31**,** 155–229.
67. Tombesi A (1994) Olive fruit growth and metabolism. *Acta Horticulturae* 356**,** 225-232.
68. Moriondo M, Orlandini, S, Nuntiis, PD, & Mandrioli, P (2001) Effect of agrometeorological parameters on the phenology of pollen emission and production of olive trees (*Olea europea* L.). *Aerobiologia* 17(3)**,** 225-232.
69. Fornaciari M, Pieroni, L, Orlandi, F, & Romano, B (2002) A new approach to consider the pollen variable in forecasting yield models. *Econ. Bot.* 56(1)**,** 66-72.
70. Ponti L, Cossu, QA, & Gutierrez, AP (2009) Climate warming effects on the *Olea europaea–Bactrocera oleae s*ystem in Mediterranean islands: Sardinia as an example. *Global Change Biol.* 15(12)**,** 2874-2884.
71. Gutierrez AP, Ponti, L, & Cossu, QA (2009) Effects of climate warming on olive and olive fly (*Bactrocera* oleae (Gmelin)) in California and Italy. *Climatic Change* 95**,** 195-217.
72. Monfreda C, Ramankutty, N, & Foley, JA (2008) Farming the planet: 2. Geographic distribution of crop areas, yields, physiological types, and net primary production in the year 2000. *Global Biogeochem. Cycles* 22**,** GB1022, DOI 1010.1029/2007GB002947.
73. Kerr JT, Kharouba, HM, & Currie, DJ (2007) The macroecological contribution to global change solutions. *Science* 316(5831)**,** 1581-1584.
74. Araújo MB, Pearson, RG, Thuiller, W, & Erhard, M (2005) Validation of species–climate impact models under climate change. *Global Change Biol.* 11(9)**,** 1504-1513.
75. Oreskes N (1998) Evaluation (not validation) of quantitative models. *Environ. Health Perspect.* 106(Suppl 6)**,** 1453-1460.
76. Heikkinen RK, et al. (2006) Methods and uncertainties in bioclimatic envelope modelling under climate change. *Progress in Physical Geography* 30(6)**,** 751–777.
77. Heikkinen RK, Marmion, M, & Luoto, M (2012) Does the interpolation accuracy of species distribution models come at the expense of transferability? *Ecography* 35(3)**,** 276-288.
78. Hulme PE (2011) Consistent flowering response to global warming by European plants introduced into North America. *Funct. Ecol.* 25(6)**,** 1189-1196.
79. Garcia-Mozo H, et al. (2009) Olive flowering phenology variation between different cultivars in Spain and Italy: modeling analysis. *Theoretical and Applied Climatology* 95(3)**,** 385-395.
80. Gonzalez Minero FJ, Candau, P, Morales, J, & Tomas, C (1998) Forecasting olive crop production based on ten consecutive years of monitoring airborne pollen in Andalusia (southern Spain). *Agric. Ecosyst. Environ.* 69(3)**,** 201-215.
81. Ribeiro H, Cunha, M, & Abreu, I (2007) Improving early-season estimates of olive production using airborne pollen multi-sampling sites. *Aerobiologia* 23(1)**,** 71-78.
82. Ribeiro H, Cunha, M, & Abreu, I (2008) Quantitative forecasting of olive yield in Northern Portugal using a bioclimatic model. *Aerobiologia* 24(3)**,** 141-150.
83. Galan C, et al. (2008) Modeling olive crop yield in Andalusia, Spain. *Agron. J.* 100(1)**,** 98-104.
84. Galan C, Vazquez, L, Garcia-Mozo, H, & Dominguez, E (2004) Forecasting olive (*Olea europaea*) crop yield based on pollen emission. *Field Crops Res.* 86(1)**,** 43-51.
85. Fornaciari M, Orlandi, F, & Romano, B (2005) Yield forecasting for olive trees. *Agron. J.* 97(6)**,** 1537-1542.

86. García-Mozo H, Perez-Badía, R, & Galán, C (2008) Aerobiological and meteorological factors' influence on olive (*Olea europaea* L.) crop yield in Castilla-La Mancha (Central Spain). *Aerobiologia* 24(1)**,** 13-18.
87. Orlandi F, et al. (2009) A comparison among olive flowering trends in different Mediterranean areas (south-central Italy) in relation to meteorological variations. *Theoretical and Applied Climatology* 97(3)**,** 339-347.
88. Ribeiro H, Santos, L, Abreu, I, & Cunha, M (2006) Influence of meteorological parameters on Olea flowering date and airborne pollen concentration in four regions of Portugal. *Grana* 45(2)**,** 115-121.
89. Oteros J, García-Mozo, H, Hervás, C, & Galán, C (2012) Biometeorological and autoregressive indices for predicting olive pollen intensity. *Int. J. Biometeorol.***,** 1-10.
90. Orlandi F, et al. (2010) Yield modelling in a Mediterranean species utilizing cause–effect relationships between temperature forcing and biological processes. *Sci. Hortic.* 123(3)**,** 412-417.
91. Minero FJG, Candau, P, Morales, J, & Tomas, C (1998) Forecasting olive crop production based on ten consecutive years of monitoring airborne pollen in Andalusia (southern Spain). *Agric. Ecosyst. Environ.* 69(3)**,** 201-215.
92. Pasternak D (2001) in *Combating Desertification with Plants*, eds Pasternak, D. & Schlissel, A. (Kluwer Academic/Plenum Publishers, New York, USA), pp 17-30.
93. Zohary D & Spiegel-Roy, P (1975) Beginnings of fruit growing in the Old World. *Science* 187(4174)**,** 319-327.
94. Blondel J (2006) The 'design' of Mediterranean landscapes: a millennial story of humans and ecological systems during the historic period. *Hum. Ecol.* 34(5)**,** 713-729.
95. Yasuda Y (1997) The raise and fall of olive cultivation in Northwestern Syria: palaeoecological study of Tell Mastuma. *Japan Review* 8**,** 251-273.
96. Renfrew JM (1973) *Palaeoethnobotany: the prehistoric food plants of the Near East and Europe* (Methuen, London, UK).
97. Lüttge U (2010) in *Desert plants: biology and biotechnology*, ed Ramawat, K. G. (Springer, Berlin, Germany), pp 461-477.
98. Pasternak D & Schlissel, A (2001) *Combating desertification with plants* (Kluwer Academic/Plenum Publishers, New York, USA).
99. Schröter D, et al. (2005) Ecosystem service supply and vulnerability to global change in Europe. *Science* 310(5752)**,** 1333-1337.
100. Geeson N, Brandt, CJ, & Thornes, JB (2002) *Mediterranean desertification: a mosaic of processes and responses* (John Wiley and Sons, Chichester, England).
101. Mtaita TA, Manqwiro, BK, & Mphuru, AN (2001) in *Combating desertification with plants*, eds Pasternak, D. & Schlissel, A. (Kluwer Academic/Plenum Publishers, New York, USA), pp 33-43.
102. de Graaff J, Duarte, F, Fleskens, L, & De Figueiredo, T (2010) The future of olive groves on sloping land and ex-ante assessment of cross compliance for erosion control. *Land Use Policy* 27(1)**,** 33-41.
103. de Graaff J, Kessler, A, & Duarte, F (2011) Financial consequences of cross-compliance and flat-rate-per-ha subsidies: The case of olive farmers on sloping land. *Land Use Policy* 28(2)**,** 388-394.
104. Fleskens L (2008) A typology of sloping and mountainous olive plantation systems to address natural resources management. *Ann. Appl. Biol.* 153(3)**,** 283-297.
105. Kosmas C, Danalatos, NG, López-Bermúdez, F, & Romero-Díaz, MA (2002) in *Mediterranean desertification: a mosaic of processes and responses*, eds Geeson, N., Brandt, C. J., & Thornes, J. B. (John Wiley and Sons, Chichester, England), pp 57-70.
106. Xiloyannis C, Martinez Raya, A, Kosmas, C, & Favia, M (2008) Semi-intensive olive orchards on sloping land: Requiring good land husbandry for future development. *J. Environ. Manage.* 89(2)**,** 110-119.
107. Loumou A & Giourga, C (2003) Olive groves: "The life and identity of the Mediterranean". *Agr. Hum. Values* 20(1)**,** 87-95.
108. Stroosnijder L, Mansinho, MI, & Palese, AM (2008) OLIVERO: The project analysing the future of olive production systems on sloping land in the Mediterranean basin. *J. Environ. Manage.* 89**,** 75-85.
109. Duarte F, Jones, N, & Fleskens, L (2008) Traditional olive orchards on sloping land: sustainability or abandonment? *J. Environ. Manage.* 89**,** 86-98.
110. Gordo O & Sanz, JJ (2010) Impact of climate change on plant phenology in Mediterranean ecosystems. *Global Change Biol.* 16(3)**,** 1082-1106.
111. Rey PJ (1995) Spatio-temporal variation in fruit and frugivorous bird abundance in olive orchards. *Ecology* 76(5)**,** 1625-1635.

112. Moriondo M, Bindi, M, Fagarazzi, C, Ferrise, R, & Trombi, G (2011) Framework for high-resolution climate change impact assessment on grapevines at a regional scale. *Reg. Environ. Change* 11(3)**,** 553-567.
113. Caffarra A & Eccel, E (2011) Projecting the impacts of climate change on the phenology of grapevine in a mountain area. *Aust. J. Grape Wine Res.* 17(1)**,** 52-61.
114. Dios-Palomares R & Martínez-Paz, JM (2011) Technical, quality and environmental efficiency of the olive oil industry. *Food Policy* 36(4)**,** 526-534.
115. Scheidel A & Krausmann, F (2011) Diet, trade and land use: a socio-ecological analysis of the transformation of the olive oil system. *Land Use Policy* 28(1)**,** 47-56.
116. Beaufoy G (2001) *The environmental impact of olive oil production in the European Union: practical options for improving the environmental impact* (European Commission, Environment Directorate-General. Available at http://ec.europa.eu/environment/agriculture/pdf/oliveoil.pdf).
117. Duarte F, Jones, N, Lucio, C, & Nunes, A (2006) The reform of the olive oil regime and its impacts on the olive and olive oil sector: a case study in Northern Portugal - Tras-os-Montes. *New Medit* 5(2)**,** 4-15.
118. Kizos T, Dalaka, A, & Petanidou, T (2010) Farmers' attitudes and landscape change: evidence from the abandonment of terraced cultivations on Lesvos, Greece. *Agr. Hum. Values* 27(2)**,** 199-212.
119. de Graaff J, Duran Zuazo, V-H, Jones, N, & Fleskens, L (2008) Olive production systems on sloping land: Prospects and scenarios. *J. Environ. Manage.* 89(2)**,** 129-139.
120. Bignal EM (1998) Using an ecological understanding of farmland to reconcile nature conservation requirements, EU agriculture policy and world trade agreements. *J. Appl. Ecol.* 35(6)**,** 949-954.
121. Rodríguez-Entrena M & Arriaza, M (2013) Adoption of conservation agriculture in olive groves: Evidences from southern Spain. *Land Use Policy* 34**,** 294-300.
122. European Commission (2013) Overview of CAP Reform 2014-2020. *Agricultural Policy Perspectives Brief,* N°5 / December 2013 http://ec.europa.eu/agriculture/policy-perspectives/policy-briefs/05_en.pdf (accessed 21 January 2014).
123. Lybbert TJ & Elabed, G (2013) An elixir for development? Olive oil policies and poverty alleviation in the Middle East and North Africa. *Development Policy Review* 31(4)**,** 485-506.
124. Infante Amate J (2012) The ecology and history of the Mediterranean olive grove: the Spanish great expansion, 1750 - 2000. *Rural History* 23(02)**,** 161-184.
125. Infante Amate J & Molina, M (2013) The socio-ecological transition on a crop scale: the case of olive orchards in southern Spain (1750–2000). *Hum. Ecol.* 41(6)**,** 961-969.
126. Infante Amate J, de Molina, MG, Vanwalleghem, T, Fernández, DS, & Gómez, JA (2013) Erosion in the Mediterranean: the case of olive groves in the South of Spain (1752–2000). *Environmental History* 18(2)**,** 360-382.
127. European Commission (2012) Economic analysis of the olive sector. *Directorate-General for Agriculture and Rural Development* http://ec.europa.eu/agriculture/olive-oil/ (accessed 21 January 2014).
128. Neteler M & Mitasova, H (2008) *Open source GIS: a GRASS GIS approach* (Springer, New York).
129. Moriondo M, Stefanini, FM, & Bindi, M (2008) Reproduction of olive tree habitat suitability for global change impact assessment. *Ecol. Model.* 218(1-2)**,** 95-109.
130. FAO, Food and Agriculture Organization of the United Nations (2001) *Global ecological zoning for the global forest resources assessment 2000: final report. Working Paper 56* (FAO, Rome, Italy).
131. Bivand R (2007) Using the R–Grass interface: current status. *OSGeo Journal* 1**,** 36-38.
132. Gutierrez AP & Baumgärtner, JU (1984) Multitrophic level models of predator-prey energetics: I. Age-specific energetics models - pea aphid *Acyrthosiphon pisum* (Homoptera: Aphididae) as an example. *Can. Entomol.* 116(7)**,** 924-932.
133. Gutierrez AP (1992) The physiological basis of ratio-dependent predator-prey theory: the metabolic pool model as a paradigm. *Ecology* 73**,** 1552-1563.
134. Gutierrez AP & Ponti, L (2013) Eradication of invasive species: why the biology matters. *Environ. Entomol.* 42(3)**,** 395-411.
135. Marcelis LFM & Heuvelink, E (2007) in *Functional-Structural Plant Modelling in Crop Production*, eds Vos, J., Marcelis, L. F. M., Visser, P. H. B. d., Struik, P. C., & Evers, J. B. (Springer, The Netherlands), pp 103-111.
136. Rodríguez D, Cure, JR, Cotes, JM, Gutierrez, AP, & Cantor, F (2011) A coffee agroecosystem model: I. Growth and development of the coffee plant. *Ecol. Model.* 222(19)**,** 3626-3639.
137. Briére JF, Pracros, P, Le Roux, AY, & Pierre, JS (1999) A novel rate model of temperature-dependent development for arthropods. *Environ. Entomol.* 28(1)**,** 22-29.

138. Sofo A, Manfreda, S, Fiorentino, M, Dichio, B, & Xiloyannis, C (2008) The olive tree: a paradigm for drought tolerance in Mediterranean climates. *Hydrol. Earth Syst. Sc.* 12(1)**,** 293-301.
139. Dichio B, Montanaro, G, Sofo, A, & Xiloyannis, C (2013) Stem and whole-plant hydraulics in olive (*Olea europaea*) and kiwifruit (*Actinidia deliciosa*). *Trees* 27(1)**,** 183-191.
140. Doupis G, Bertaki, M, Psarras, G, Kasapakis, I, & Chartzoulakis, K (2013) Water relations, physiological behavior and antioxidant defence mechanism of olive plants subjected to different irrigation regimes. *Sci. Hortic.* 153**,** 150-156.
141. Artale V, et al. (2010) An atmosphere-ocean regional climate model for the Mediterranean area: assessment of a present climate simulation. *Clim. Dynam.* 35(5)**,** 721-740.
142. Abdi H (2010) in *Encyclopedia of Research Design*, ed Salkind, N. (SAGE Publications, housand Oaks, California, USA), pp 169-171.
143. Martin JD & Gray, LN (1971) Measurement of relative variation: Sociological examples. *American Sociological Review* 36(3)**,** 496-502.
144. Livers JJ (1942) Some limitations to use of coefficient of variation. *Journal of Farm Economics* 24(4)**,** 892-895.
145. Vermoere M, Vanhecke, L, Waelkens, M, & Smets, E (2003) Modern and ancient olive stands near Sagalassos (south-west Turkey) and reconstruction of the ancient agricultural landscape in two valleys. *Global Ecol. Biogeogr.* 12(3)**,** 217-235.
146. Wickham H (2009) *ggplot2: elegant graphics for data analysis* (Springer, New York, USA).
147. Hodge V & Austin, J (2004) A survey of outlier detection methodologies. *Artif. Intell. Rev.* 22(2)**,** 85-126.
148. Laurikkala J, Juhola, M, & Kentala, E (2000) in *Fifth International Workshop on Intelligent Data Analysis in Medicine and Pharmacology IDAMAP-2000 Berlin, Germany, 22 August 2000. Aworkshop of the 14th European Conference on Artificial Intelligence ECAI-2000*, eds Lavrac, N., Miksch, S., & Kavsek, B., pp 20-24.
149. Tominski C, Fuchs, G, & Schumann, H (2008) Task-driven color coding. *Information Visualisation, 2008. IV '08. 12th International Conference, 9-11 July 2008, London, UK***,** http://dx.doi.org/10.1109/IV.2008.1124.
150. Abdel-Razik M (1989) A model of the productivity of olive trees under optional water and nutrient supply in desert conditions. *Ecol. Model.* 45(3)**,** 179-204.
151. Gutierrez AP, Falcon, LA, Loew, W, Leipzig, PA, & van-den Bosch, R (1975) An analysis of cotton production in California: a model for acala cotton and the effects of defoliators on its yields. *Environ. Entomol.* 4(1)**,** 125-136.
152. Gutierrez AP, Baumgärtner, JU, & Summers, CG (1984) Multitrophic level models of predator-prey energetics: III. A case study of an alfalfa ecosystem. *Can. Entomol.* 116(7)**,** 950-963.
153. Gutierrez AP, Pitcairn, MJ, Ellis, CK, Carruthers, N, & Ghezelbash, R (2005) Evaluating biological control of yellow starthistle (*Centaurea solstitialis*) in California: A GIS based supply-demand demographic model. *Biol. Control* 34(2)**,** 115-131.
154. Gilioli G & Cossu, A (2002) First validation of an individual-based model for the population dynamics of *Bactrocera oleae* (Gmelin). *Atti XIX Congresso Nazionale di Entomologia, Catania, 10-15 giugno 2002***,** 34-39.
155. Vansickle J (1977) Attrition in distributed delay models. *IEEE T. Syst. Man, Cyb.* 7**,** 635-638.
156. Di Cola G, Gilioli, G, & Baumgärtner, J (1999) in *Ecol. Entomol.*, eds Huffaker, C. B. & Gutierrez, A. P. (John Wiley and Sons, New York), pp 503-534.
157. de Wit CT & Goudriaan, J (1978) *Simulation of ecological processes* (PUDOC Publishers, The Netherlands).
158. Watt KEF (1959) A mathematical model for the effects of densities of attacked and attacking species on the number attacked. *Can. Entomol.* 91**,** 129-144.
159. Fletcher BS & Kapatos, ET (1983) in *Fruit flies of economic importance Proceedings of the CEC/IOBC International Symposium, Athens, Greece, 16 19 November 1982. 1983; 321 329* (Rotterdam Netherlands: A.A. Balkema.).
160. Koveos DS (2001) Rapid cold hardening in the olive fruit fly *Bactrocera oleae* under laboratory and field conditions. *Entomol. Exp. Appl.* 101(3)**,** 257-263.
161. Denney JO, McEachern, GR, & Griffiths, JF (1985) Modeling the thermal adaptability of the olive (*Olea europaea* L.) in Texas. *Agric. For. Meteorol.* 35(1-4)**,** 309.
162. Fernandez JE & Moreno, F (1999) Water use by the olive tree. *J. Crop Prod.* 2(2)**,** 101-162.
163. Tubeileh A, Bruggeman, A, & Turkelboom, F (2009) Effect of water harvesting on growth of young olive trees in degraded Syrian dryland. *Environ. Dev. Sustainability* 11(5)**,** 1073-1090.

164. FAO, Food and Agriculture Organization of the United Nations & IIASA, International Institute for Applied Systems Analysis (2011) *Global Agro-ecological Zones (GAEZ v3.0)* (FAO Rome, Italy and IIASA, Laxenburg, Austria).

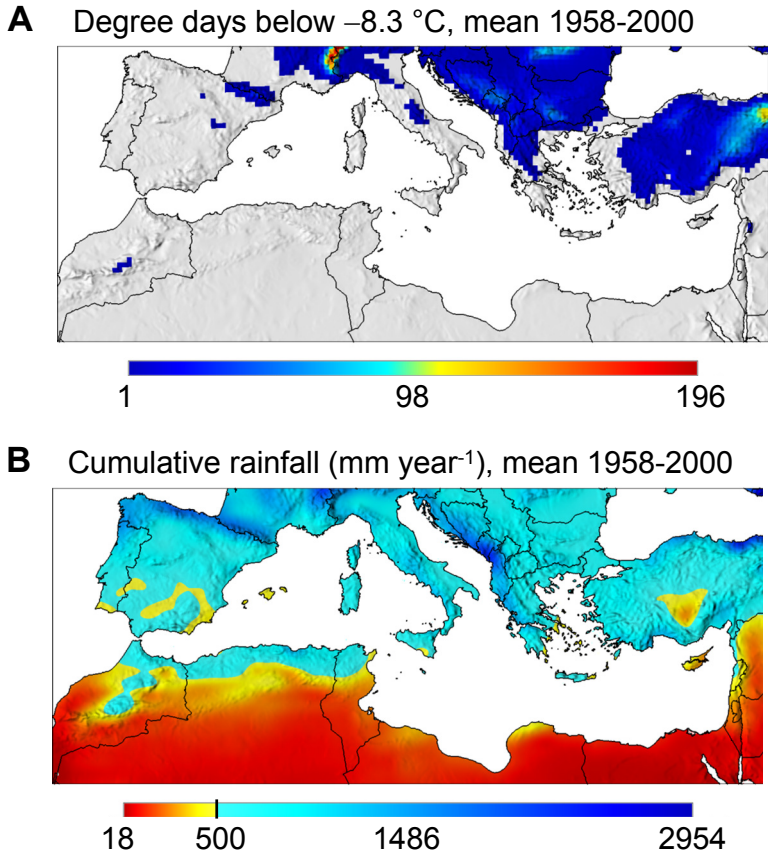

Fig. S1. Climatic favorability for olive in the Mediterranean Basin. Mean degree days ≤ –8.3 °C (freeze damage threshold for olive) (161) (A), and mean yearly rainfall (mm y^{-1}) (B) for the period 1958-2000 based on daily weather from the ERA40 reanalysis of meteorological observations downscaled to a 30 km grid (141). The reference precipitation value of 500 mm y^{-1} in (B) is the lower limit for commercial yields under rain fed conditions (162) while rain <350 mm y^{-1} defines the lower limit of olive distribution in arid areas (163).

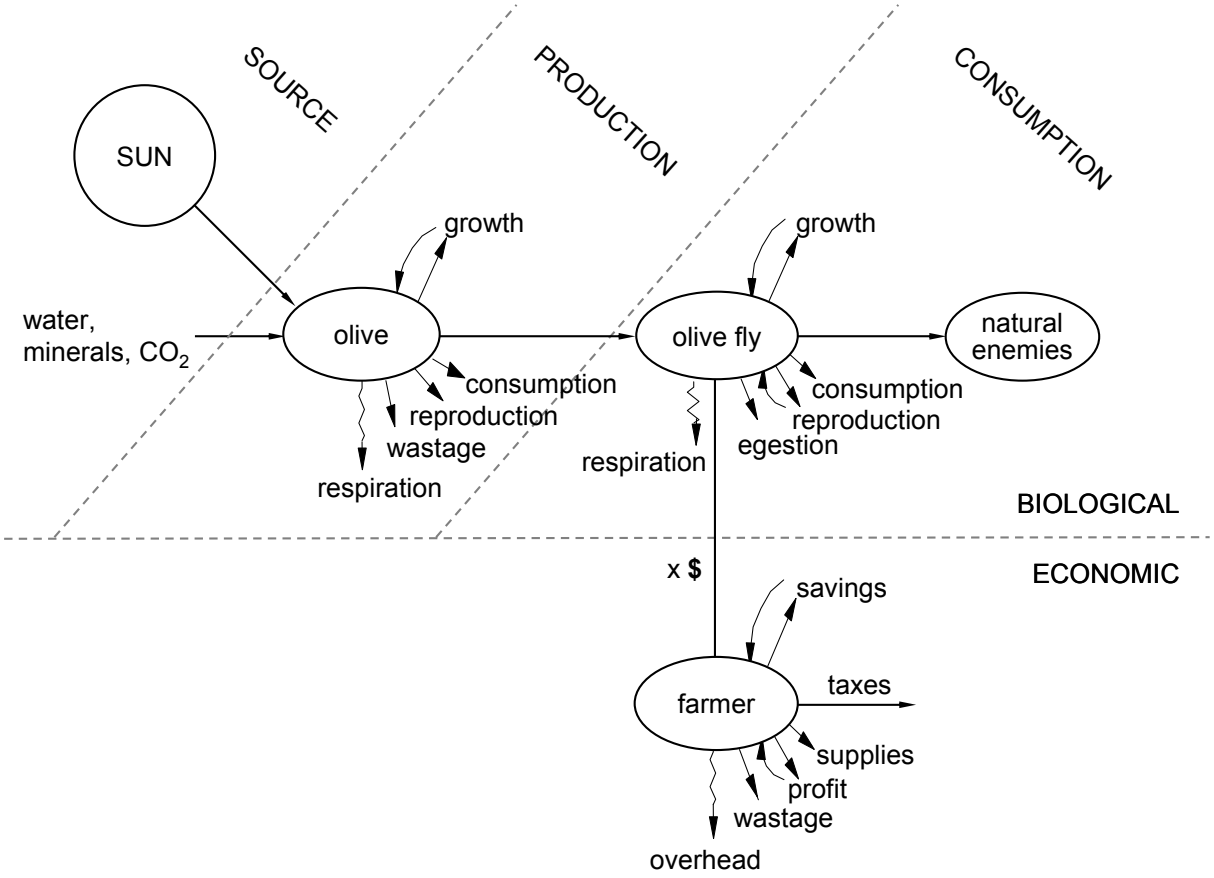

Fig. S2. Multitrophic mass (i.e., energy) flow in the consumer-resource population dynamics model as applied to the olive eco-social system (see refs. 40, 42, 43); the symbol $ indicates the conversion of the mass/energy flow into monetary units.

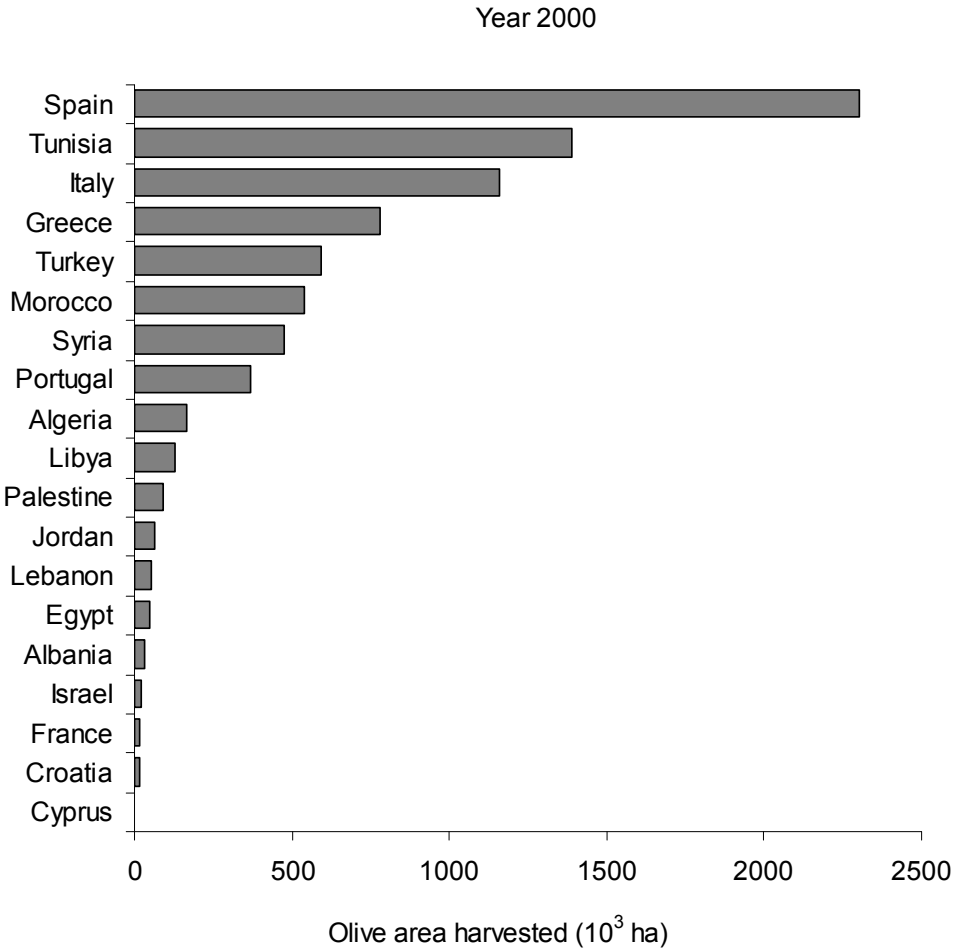

Fig. S3. Olive crop area in countries of the Mediterranean Basin. Data from FAOSTAT refers to the year 2000, the same reference year used to derive the olive distribution map in Fig. 2A.

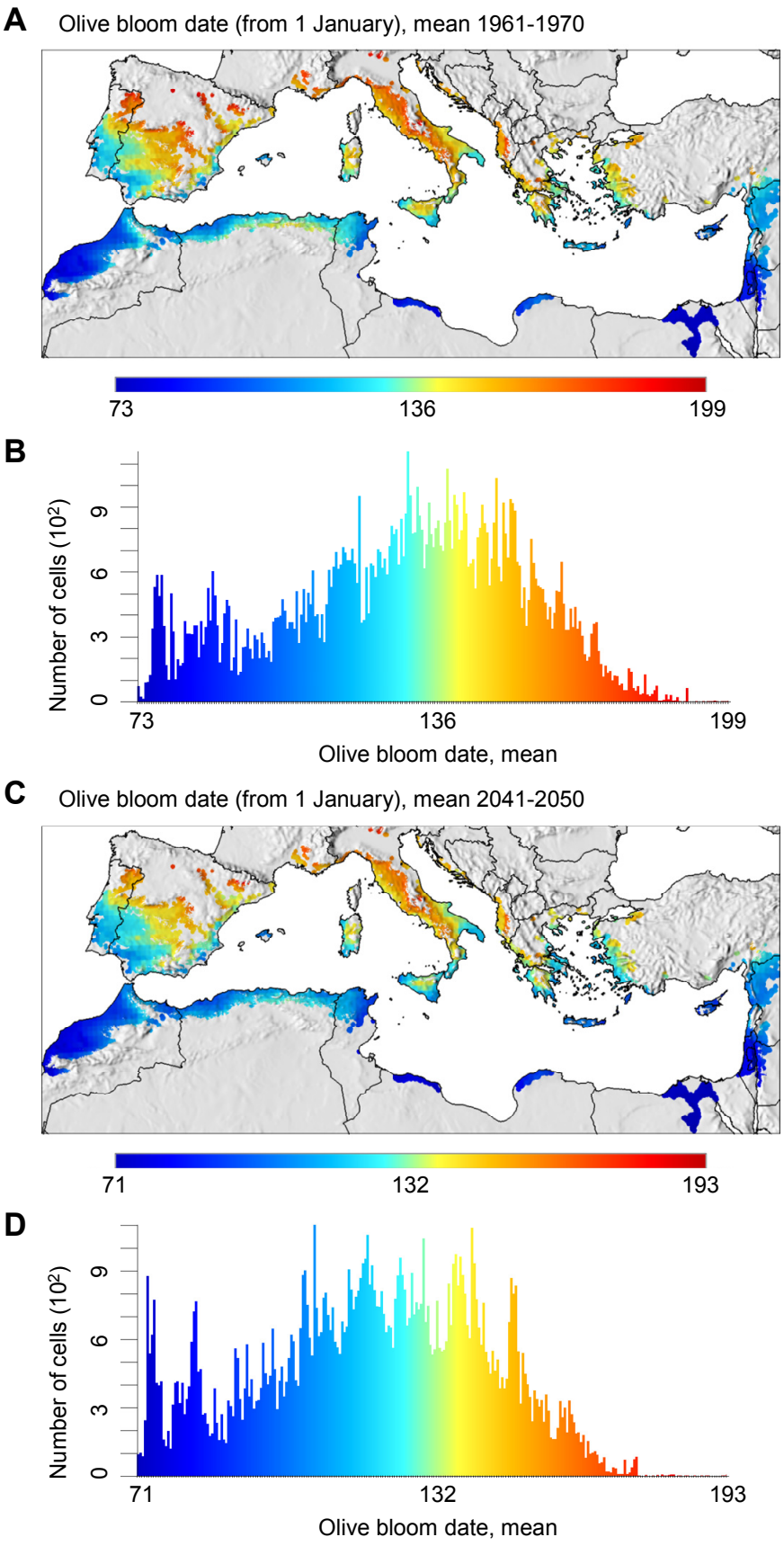

Fig. S4. Mean of olive bloom date (days from 1 January) under the A1B +1.8°C climate warming scenario. Map (A) and frequency histogram (B) for the period 1961-1970; and map (C) and frequency histogram (D) for the period 2041-2050.

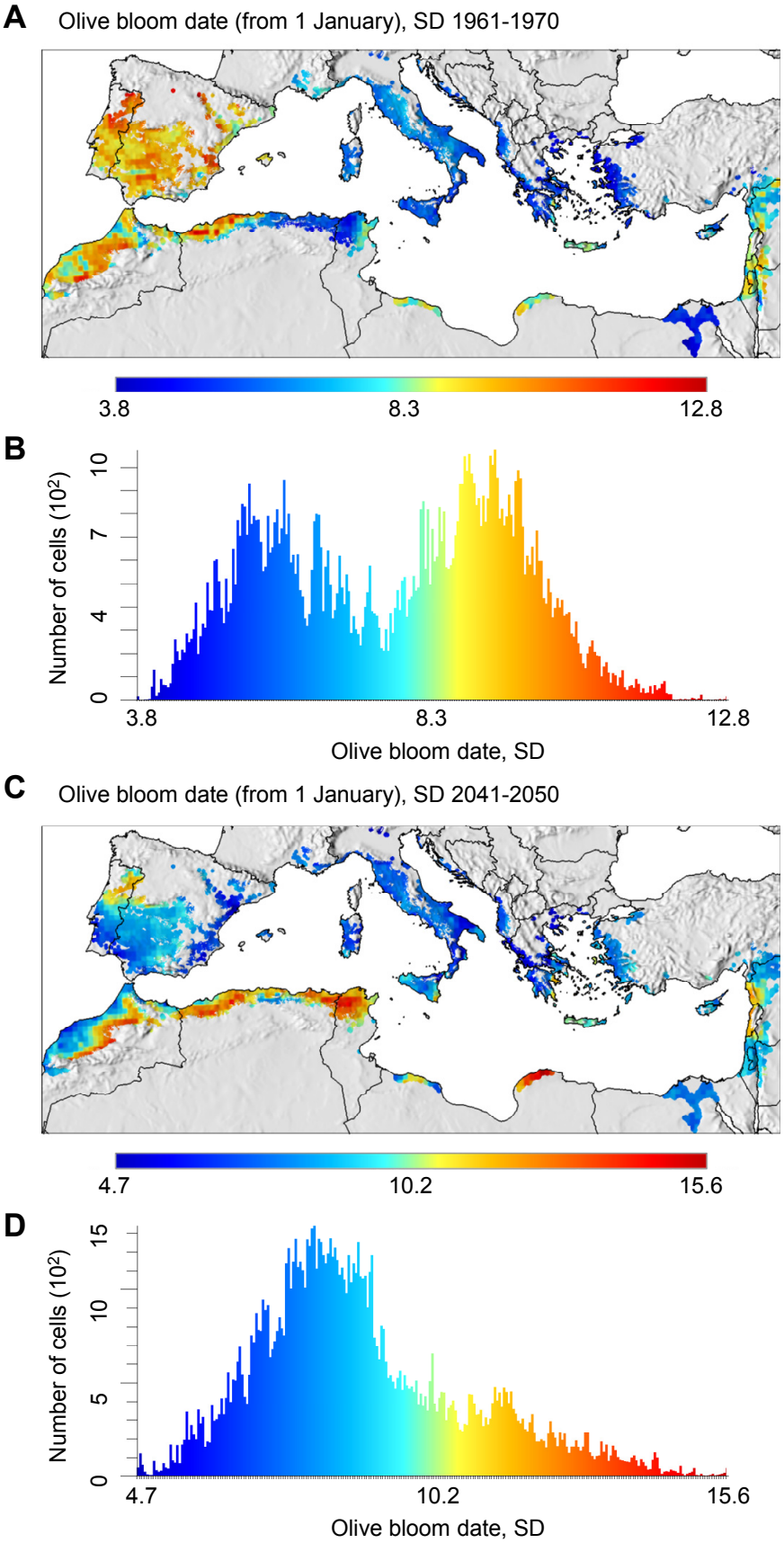

Fig. S5. Standard deviation (SD) of olive bloom date (days from 1 January) under the A1B +1.8°C climate warming scenario. Map (A) and frequency histogram (B) for the period 1961-1970; and map (C) and frequency histogram (D) for the period 2041-2050.

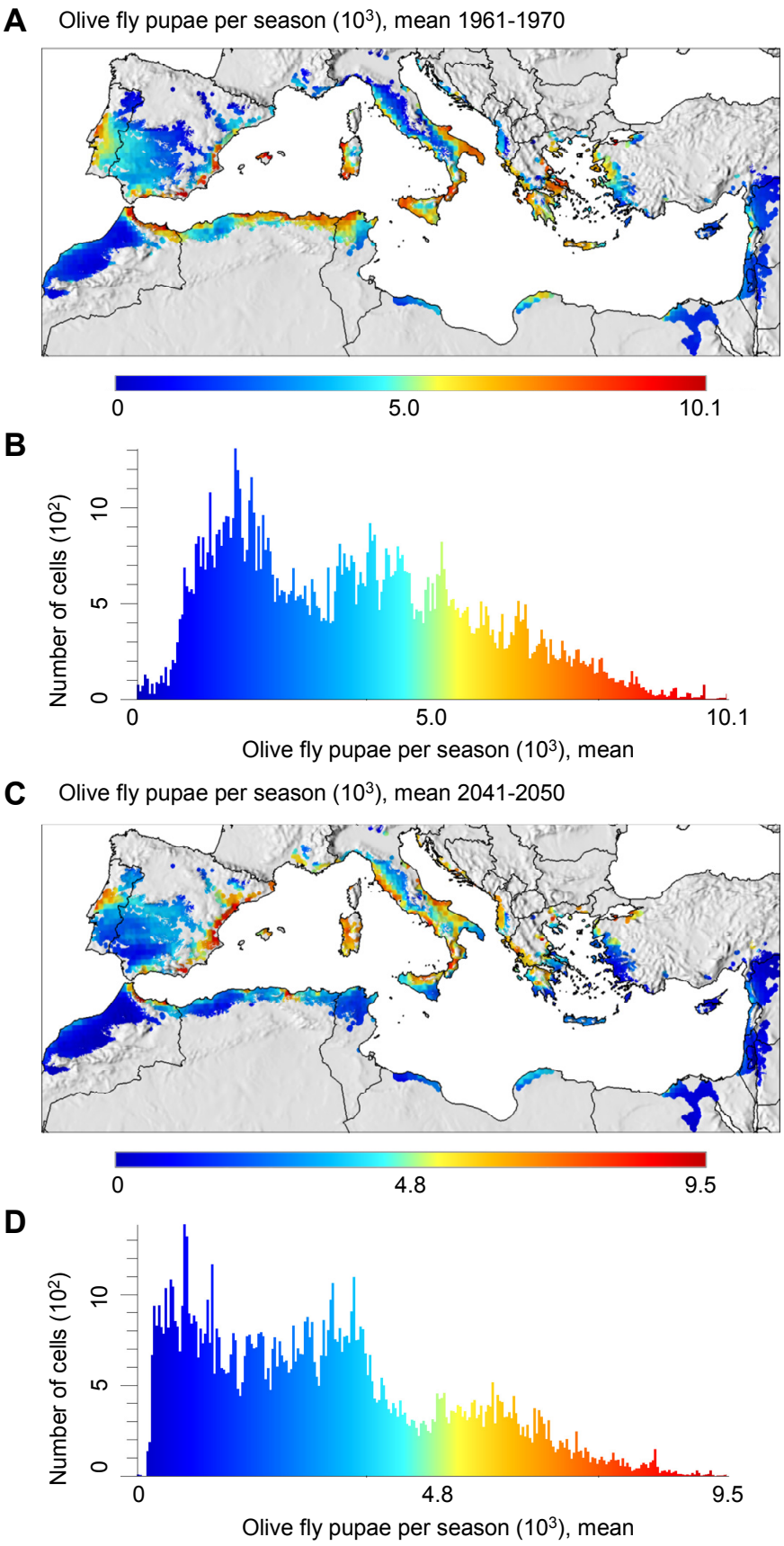

Fig. S6. Mean of olive fly abundance (cumulative pupae × 10^3 season^{-1} tree^{-1}) under the A1B +1.8°C climate warming scenario. Map (A) and frequency histogram (B) for the period 1961-1970; and map (C) and frequency histogram (D) for the period 2041-2050.

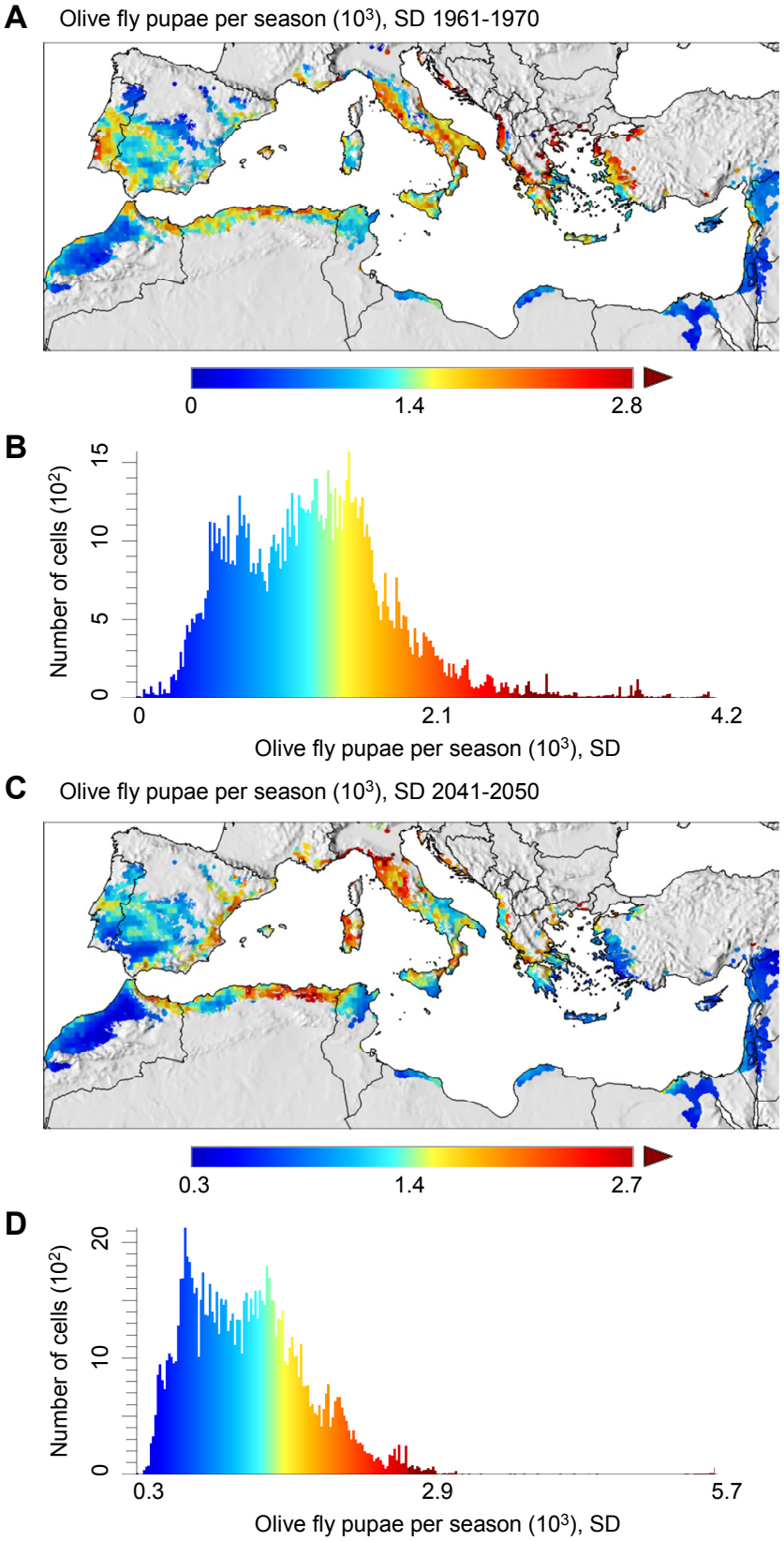

Fig. S7. Standard deviation (SD) of olive fly abundance (cumulative pupae $\times$ 10^3 season^{-1} tree^{-1}) under the A1B +1.8°C climate warming scenario. Map (A) and frequency histogram (B) for the period 1961-1970; and map (C) and frequency histogram (D) for the period 2041-2050. Outliers identified using R boxplot function. Full data intervals are [0, 4.2] (A, B) and [0.3, 5.7] (C, D).

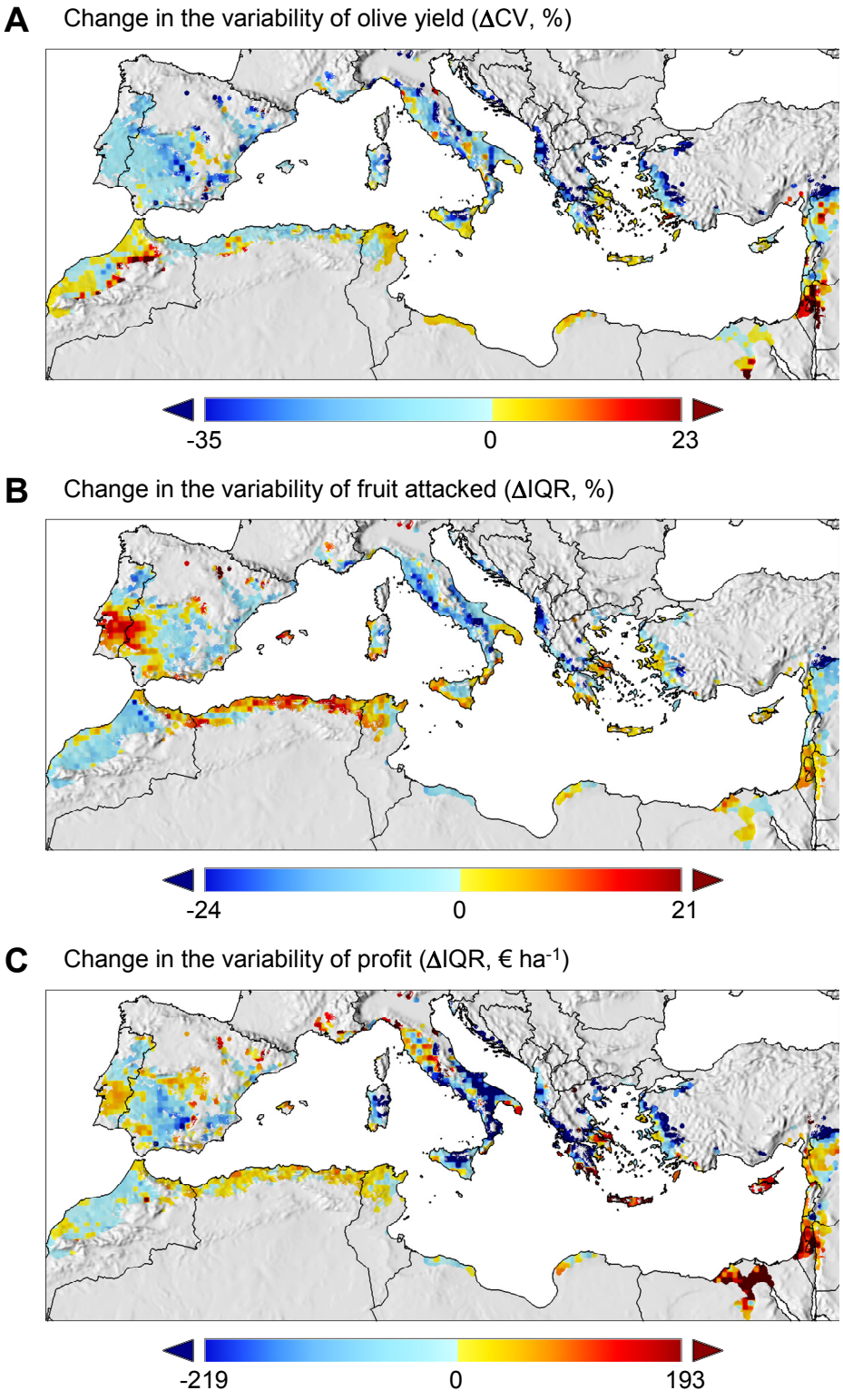

Fig. S8. Risk change in olive production induced by bio-economic multitrophic effects of climate warming in the Mediterranean Basin. Change (Δ) in the variability of (A) the coefficient of variation (CV, %) of olive yield, (B) the interquartile range (IQR, see SI Methods) of fruit infestation by olive fly (%), and (C) the IQR of profit (€ ha^{-1}) as driven by the A1B +1.8°C climate warming scenario. Outliers were identified using R boxplot function. Full data intervals are [-134, 275.4] (A), [-42.8, 23.7] (B), and [-1,832.0, 991.6] (C).

Fig. S9. Sub-regions of the Mediterranean Basin used in Fig. 6 and Table 1 (color palette from http://colorbrewer2.org/).

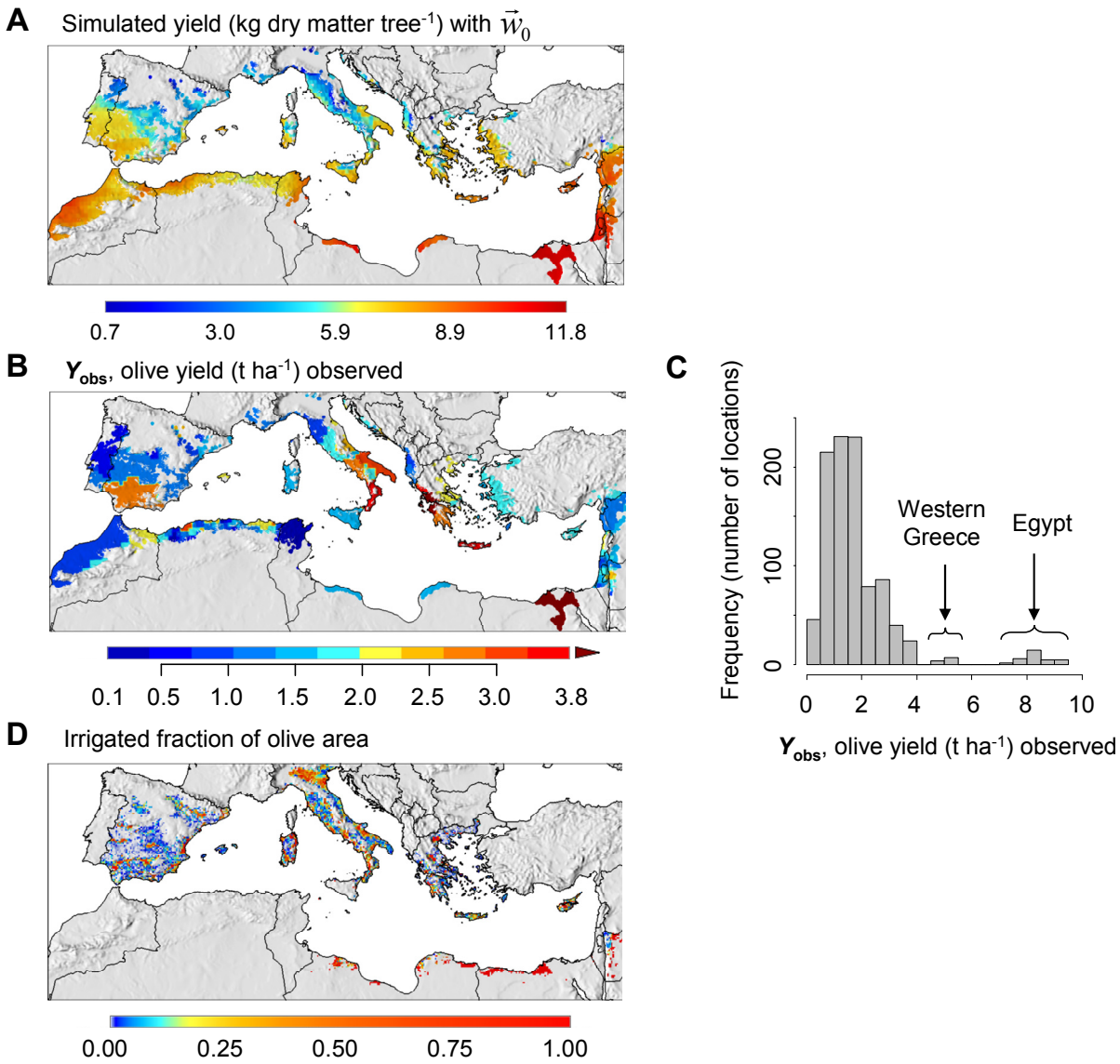

Fig. S10. Simulated and observed olive yield in the Mediterranean Basin. (A) Map of simulated yield with baseline weather $\vec{w}_0$ (kg dry matter tree^{-1}; mean for years 1961-1970). (B) Map of observed yield (t ha^{-1}; mean for years 1997-2003) where values >3.8 are shown as outliers for presentation purposes (outliers identified using R boxplot function). (C) Frequency histogram of yields shown in (B) with indication of bars for Western Greece and Egypt (i.e., the data shown as outliers in subpanel B). (D) Fraction of harvested olive area subject to irrigation on a 10 x 10 km pixel base (164). Note that simulated patterns capture higher-than-average yields in areas such as Spain (Andalucía district), Egypt, Greece and southern Italy, while in other areas such as North Africa, the rest of the Middle East and Turkey simulated yield appear high relative to observed records as a results of a mix of factors including the lack of irrigation and a combination of other agronomic practices. In addition, simulated yield is expressed as fruit dry matter per plant whereas observed yield is fresh fruit per unit area, and hence factors such as planting density and the presence of table olives (with higher water content at harvest than olives used for oil production) may both contribute to widen the difference between simulated and observed yields. This suggests that using the physiological response of olive to weather for scaling observed yield is a robust approach to mechanistic analysis of the olive system at the scale of the Mediterranean Basin.